

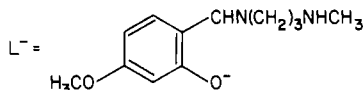
Contribution from the Dipartimento di Chimica and Dipartimento di Scienze della Terra, Sezione Cristallografia, Università di Perugia, 06100 Perugia, Italy

## Exchange Interaction in Multinuclear Transition-Metal Complexes. 7.<sup>1</sup> Synthesis, X-ray Structure, and Magnetic Properties of $\text{Cu}_3\text{L}_2(\text{CH}_3\text{COO})_4$ (LH = *N*-Methyl-*N'*-(4-methoxysalicylidene)-1,3-propanediamine), a Novel Linear Trinuclear Copper(II) Compound

B. Chiari, O. Piovesana,\* T. Tarantelli, and P. F. Zanazzi

Received April 8, 1985

The synthesis, crystal structure, and magnetic properties are reported for the novel compound  $\text{Cu}_3\text{L}_2(\text{CH}_3\text{COO})_4$ , where  $\text{L}^-$  is the tridentate anion of *N*-methyl-*N'*-(4-methoxysalicylidene)-1,3-propanediamine. The compound  $\text{C}_{32}\text{H}_{46}\text{N}_4\text{O}_{12}\text{Cu}_3$  crystallizes



in the triclinic system, space group  $P\bar{1}$ , with  $Z = 1$ . Lattice constants:  $a = 10.865$  (3),  $b = 10.852$  (3),  $c = 7.768$  (3) Å;  $\alpha = 88.03$  (2),  $\beta = 95.86$  (2),  $\gamma = 97.49$  (2)°. Least-squares refinement of 1070 observed reflections and 155 parameters led to a final  $R(\text{weighted})$  factor of 0.042. The structure of the complex consists of strictly linear trimers of Cu atoms. The chromophores of the central ( $\text{CuO}_6$ ) and outer ( $\text{CuN}_2\text{O}_3$ ) copper atoms have different geometries, elongated octahedral and distorted trigonal bipyramidal, respectively. Adjacent copper atoms are linked by both  $\text{Cu}-\text{O}-\text{C}-\text{O}-\text{Cu}$  and  $\text{Cu}_2\text{O}_2$  bridges. Variable-temperature magnetic susceptibility data, in the range 2–300 K, have been fit by using a Hamiltonian containing two  $J$  parameters, one pertaining to the interaction between adjacent copper atoms and the other to the interaction between the outer copper atoms. Difficulties in obtaining meaningful values of the spin-Hamiltonian parameters for trinuclear species are discussed. The results for this trimer clearly indicate a weak antiferromagnetic coupling ( $-J$  ca. 5–10  $\text{cm}^{-1}$ ) between nearest neighbors but do not provide reliable information on the end-to-end interaction. The magnitude and nature of the antiferromagnetic coupling that is observed between nearest neighbors are interpreted in terms of the orbital pathways that are available for exchange and compared with those pertaining to cupric carboxylates with a bridged dinuclear structure.

### Introduction

The magnetic properties of exchange-coupled dinuclear copper(II) compounds have been examined extensively.<sup>2</sup> The theory appropriate for such systems is found generally adequate for the description of the magnetic properties and, in particular, usually allows accurate values of the exchange parameters to be deduced from experimental data. These accurate values have provided an invaluable basis for e.g. the foundation of magnetostructural correlations<sup>2a,b</sup> and the elucidation of superexchange mechanisms.<sup>2c,d,3</sup>

Exchange interactions in trinuclear copper(II) compounds, particularly linear compounds, appear to be much less understood than those pertaining to dimeric species, mainly because of the inherent greater difficulties in comparing theory with experiment<sup>4-9</sup> and the paucity of suitably documented complexes that are available.<sup>2,8-11</sup>

Especially in light of the effort that is being made to extend the concept of magnetostructural correlation from dimeric to polymeric systems,<sup>2a,e</sup> a deeper insight into the magnetic and structural properties of trinuclear compounds, the first step on passing from the former to the latter species, appears highly desirable.

Here we report the synthesis and X-ray structural and magnetic analyses of a novel trinuclear copper(II) system, this being  $\text{Cu}_3\text{L}_2(\text{CH}_3\text{COO})_4$ , where LH is the tridentate Schiff base *N*-methyl-*N'*-(4-methoxysalicylidene)-1,3-propanediamine. The compound is of interest since it proves to be the first example of a linear trimer with both  $\text{Cu}-\text{O}-\text{Cu}$  and  $\text{Cu}-\text{O}-\text{C}-\text{O}-\text{Cu}$  acetate bridges and since its magnetic behavior clearly shows the effects of the population of the quartet and doublet states. To the best of our knowledge, only one example of such magnetic behavior has been previously reported.<sup>9</sup>

### Experimental Section

**Preparation of the Complex.** A solution of the new ligand LH was prepared by adding a 20-mL portion of a 0.50 M solution of 2-hydroxy-4-methoxybenzaldehyde in carefully dried and deoxygenated

ethanol to a 0.33 M solution (30 mL) of *N*-methyl-1,3-propanediamine in the same solvent. The addition was made at ca. 50 °C, with constant stirring and, as with all subsequent manipulations, in a dry-nitrogen atmosphere. The reaction mixture was heated under reflux for 30 min, with stirring, and then cooled at room temperature. A 2.0-g (0.01-mol) quantity of  $\text{Cu}(\text{CH}_3\text{COO})_2 \cdot \text{H}_2\text{O}$  was added to the solution of the LH ligand. The addition was made over a period of 30 min, with constant stirring. The reaction mixture was then stirred for an additional 15 min. A clear, dark green solution was obtained. After ca. 12 h of standing at room temperature, a green, crystalline precipitate of the complex was collected by filtration in a dry-nitrogen atmosphere and dried under vacuum: yield 1 g (35%); mp 199–201 °C. Anal. Calcd for  $\text{C}_{32}\text{H}_{46}\text{N}_4\text{O}_{12}\text{Cu}_3$ : C, 44.21; H, 5.33; N, 6.44; Cu, 21.93. Found: C, 44.17; H, 5.11, N, 6.54; Cu, 21.48. The compound is slightly air-sensitive. However, the decomposition process takes several days (ca. 10) to become perceptible.

**Magnetic Measurements.** The magnetic susceptibilities were measured on a Faraday balance between 77 K and room temperature. Measurements between ca. 2 and 60 K were obtained with use of a Princeton Applied Research Model 155 vibrating-sample magnetometer operating at 10 kG, as described elsewhere.<sup>12</sup> Susceptibilities were corrected for

- (1) Part 6: Chiari, B.; Piovesana, O.; Tarantelli, T.; Zanazzi, P. F. *Inorg. Chem.* **1984**, *23*, 3398.
- (2) For reviews see: (a) Hatfield, W. E. In "Magneto-Structural Correlations in Exchange Coupled Systems"; Willett, R. D., Gatteschi, D., Kahn, O., Eds.; D. Reidel Publishing Co.: Dordrecht, 1985; p 555. (b) Willett, R. D. *Ibid.*, p 389. (c) Kahn, O. *Ibid.*, p 37. (d) Hendrickson, D. N. *Ibid.*, p 523. (e) de Jongh, L. J. *Ibid.*, p 1. (f) Gatteschi, D.; Bencini, A. *Ibid.*, p 241.
- (3) Hay, P. J.; Thibeault, J. C.; Hoffmann, R. *J. Am. Chem. Soc.* **1975**, *97*, 4884.
- (4) Jotham, W. R.; Kettle, F. A.; Marks, J. A. *J. Chem. Soc., Faraday Trans. 2* **1976**, 125 and references therein.
- (5) Gruber, S. J.; Harris, C. M.; Sinn, E. *J. Chem. Phys.* **1968**, *49*, 2183.
- (6) Epstein, J. M.; Figgis, B. N.; White, A. H.; Willis, A. C. *J. Chem. Soc., Dalton Trans.* **1974**, 1954.
- (7) Figgis, B. N.; Martin, D. J. *J. Chem. Soc., Dalton Trans.* **1972**, 2174.
- (8) Banci, L.; Bencini, A.; Gatteschi, D. *Inorg. Chem.* **1983**, *22*, 2681.
- (9) Butcher, R. J.; O'Connor, C. J.; Sinn, E. *Inorg. Chem.* **1981**, *20*, 537.
- (10) Brown, D. A.; Wasson, J. R.; Hall, J. W.; Hatfield, W. E. *Inorg. Chem.* **1977**, *16*, 2526 and reference therein.
- (11) Fletcher, R.; Hansen, J. J.; Livermore, J.; Willett, R. D. *Inorg. Chem.* **1983**, *22*, 330.
- (12) Hall, J. W.; Marsh, W. E.; Weller, R. R.; Hatfield, W. E.; *Inorg. Chem.* **1981**, *20*, 1033 and references therein.

\* To whom correspondence should be addressed at the Dipartimento di Chimica.

**Table I.** Fractional Atomic Coordinates<sup>a</sup> in  $\text{Cu}_3\text{L}_2(\text{CH}_3\text{COO})_4$ 

atom	<i>x/a</i>	<i>y/b</i>	<i>z/c</i>
Cu(1)	0.5000	0.5000	0.5000
Cu(2)	0.3614 (1)	0.7529 (1)	0.5252 (2)
O(1)	0.5294 (6)	0.7228 (6)	0.5991 (9)
O(2)	0.3330 (6)	0.5329 (6)	0.5608 (9)
O(3)	0.3933 (6)	0.7377 (6)	0.2683 (8)
O(4)	0.4514 (6)	0.5430 (6)	0.2600 (8)
O(5)	0.1643 (7)	0.5171 (7)	0.7002 (10)
O(6)	0.9325 (7)	0.7708 (7)	0.9104 (10)
N(1)	0.3789 (8)	0.9154 (8)	0.6504 (10)
N(2)	0.1749 (8)	0.7319 (8)	0.4771 (11)
C(1)	0.6120 (5)	0.7904 (6)	0.7078 (9)
C(2)	0.7242 (5)	0.7424 (6)	0.7532 (9)
C(3)	0.8204 (5)	0.8115 (6)	0.8549 (9)
C(4)	0.8044 (5)	0.9286 (6)	0.9111 (9)
C(5)	0.6922 (5)	0.9765 (6)	0.8657 (9)
C(6)	0.5960 (5)	0.9074 (6)	0.7640 (9)
C(7)	0.4834 (10)	0.9635 (10)	0.7356 (14)
C(8)	0.2747 (10)	0.9916 (10)	0.6416 (15)
C(9)	0.1494 (10)	0.9134 (10)	0.6585 (14)
C(10)	0.1038 (10)	0.8394 (10)	0.4998 (14)
C(11)	0.1266 (12)	0.6705 (11)	0.3110 (15)
C(12)	0.4167 (9)	0.6413 (10)	0.1939 (14)
C(13)	0.3987 (12)	0.6506 (11)	0.0006 (15)
C(14)	0.2544 (10)	0.4712 (10)	0.6524 (14)
C(15)	0.2697 (11)	0.3352 (10)	0.7063 (16)
C(16)	0.9503 (12)	0.6427 (11)	0.8719 (17)

<sup>a</sup> Estimated standard deviations in parentheses refer to the last digit in this and the following table.

the diamagnetism of the ligand system ( $-126 \times 10^{-6}$  cgsu/Cu atom). The results were evaluated by using standard least-squares minimization computer programs. Our analysis used a temperature-independent paramagnetic term,  $N\alpha$ , of zero and did not include any zero-field splitting.

**ESR Spectra.** These were measured with a Varian E-109 spectrometer operated at X-band frequency and with diphenylpicrylhydrazyl (DPPH) as internal reference.

**X-ray Data and Structure Solution.** A green, tabular crystal with dimensions  $0.14 \times 0.14 \times 0.03$  mm was mounted on a computer-controlled Philips PW1100 single-crystal diffractometer, equipped with graphite-monochromatized Mo  $K\alpha$  radiation ( $\lambda = 0.71069$  Å). The crystals are triclinic. The cell dimensions, determined by a least-squares calculation based on the setting angles of 25 selected reflections, are  $a = 10.865$  (3) Å,  $b = 10.852$  (3) Å,  $c = 7.768$  (3) Å,  $\alpha = 88.03$  (2)°,  $\beta = 95.86$  (2)°,  $\gamma = 97.49$  (2)°, and  $V = 903.1$  Å<sup>3</sup>. The space group is  $P\bar{1}$ , as confirmed by the structural analysis. The calculated density for one molecule of  $\text{C}_{32}\text{H}_{46}\text{N}_4\text{O}_{12}\text{Cu}_3$  (mol wt = 868.5) in the unit cell is  $1.596$  g cm<sup>-3</sup>; the absorption coefficient for Mo  $K\alpha$  is  $\mu = 18.20$  cm<sup>-1</sup>. The intensity data were collected in the range  $4^\circ \leq 2\theta \leq 42^\circ$ ; the  $\omega$ - $2\theta$  scan technique was employed, the scan range being  $1.4^\circ$  and the speed  $0.04^\circ$  s<sup>-1</sup>. A total of 2995 independent reflections were measured (at room temperature), of which 1925 having  $I < 3\sigma(I)$  were considered as "unobserved" and excluded from the refinement. Three standard reflections were measured periodically and showed no apparent variation in intensity during data collection. The data were corrected for Lorentz and polarization factors. An empirical absorption correction was applied during the refinement, according to the method of Walker and Stuart.<sup>13</sup> The correction factors were in the range 1.22–0.98.

The structure was solved by the Patterson method and refined by the full-matrix least-squares method with the SHELX-76 package of programs.<sup>14</sup> The function minimized was  $\sum w(|F_o| - |F_c|)^2$ . The phenyl groups were constrained to perfect hexagons (C–C = 1.395 Å) and refined as rigid groups. The hydrogen atoms (with the exception of those of the methyl groups) were included at their calculated positions (C–H = 1.08 Å) with overall isotropic parameter  $U = 0.06$  Å<sup>2</sup>. The methyl groups were refined as rigid groups starting from the staggered position. Anisotropic thermal parameters were refined for the Cu, O, and N atoms. The refinement covered at  $R(\text{unweighted}) = 0.043$  and  $R(\text{weighted}) = 0.042$ , for 155 parameters and 1070 observed reflections ( $R_w = (\sum w(|F_o| - |F_c|)^2)^{1/2} / (\sum wF_o^2)^{1/2}$ ,  $w = (\sigma^2(F_o) + 0.0004F_o^2)^{-1}$ ). The atomic scattering factors were taken from ref 14 for O, N, C, and H and from ref

**Table II.** Bond Lengths (Å) and Angles (deg) in  $\text{Cu}_3\text{L}_2(\text{CH}_3\text{COO})_4$ 

Cu(1)–O(1)	2.533 (7)	O(6)–C(3)	1.373 (8)
Cu(1)–O(2)	2.000 (5)	O(6)–C(16)	1.473 (14)
Cu(1)–O(4)	1.943 (6)	N(1)–C(7)	1.310 (12)
Cu(2)–O(1)	1.923 (5)	N(1)–C(8)	1.481 (12)
Cu(2)–O(2)	2.377 (7)	N(2)–C(10)	1.505 (13)
Cu(2)–O(3)	2.076 (6)	N(2)–C(11)	1.488 (14)
Cu(2)–N(1)	2.021 (9)	C(6)–C(7)	1.430 (10)
Cu(2)–N(2)	2.007 (7)	C(8)–C(9)	1.523 (13)
O(1)–C(1)	1.331 (9)	C(9)–C(10)	1.500 (15)
O(2)–C(14)	1.275 (12)	C(12)–C(13)	1.496 (16)
O(3)–C(12)	1.278 (12)	C(14)–C(15)	1.545 (16)
O(4)–C(12)	1.254 (12)	Cu(1)–Cu(2)	3.319 (1)
O(5)–C(14)	1.248 (11)		
O(1)–Cu(1)–O(2)	74.2 (2)	Cu(2)–N(1)–C(7)	122.9 (6)
O(1)–Cu(1)–O(4)	94.3 (2)	Cu(2)–N(1)–C(8)	121.3 (5)
O(2)–Cu(1)–O(4)	89.4 (2)	C(7)–N(1)–C(8)	115.7 (7)
O(1)–Cu(2)–O(2)	79.3 (2)	Cu(2)–N(2)–C(10)	120.0 (5)
O(1)–Cu(2)–O(3)	90.5 (2)	Cu(2)–N(2)–C(11)	114.5 (5)
O(1)–Cu(2)–N(1)	93.7 (2)	C(10)–N(2)–C(11)	109.2 (7)
O(1)–Cu(2)–N(2)	162.6 (2)	O(1)–C(1)–C(2)	115.9 (4)
O(2)–Cu(2)–O(3)	90.9 (2)	O(1)–C(1)–C(6)	123.9 (4)
O(2)–Cu(2)–N(1)	144.4 (2)	O(6)–C(3)–C(2)	124.3 (4)
O(2)–Cu(2)–N(2)	84.0 (2)	O(6)–C(3)–C(4)	115.7 (4)
O(3)–Cu(2)–N(1)	124.3 (2)	C(1)–C(6)–C(7)	125.4 (5)
O(3)–Cu(2)–N(2)	94.6 (2)	C(5)–C(6)–C(7)	114.5 (5)
N(1)–Cu(2)–N(2)	97.1 (3)	N(1)–C(7)–C(6)	126.2 (7)
Cu(1)–O(1)–Cu(2)	95.3 (2)	N(1)–C(8)–C(9)	112.5 (7)
Cu(1)–O(1)–C(1)	135.1 (3)	C(8)–C(9)–C(10)	112.2 (7)
Cu(2)–O(1)–C(1)	127.0 (4)	N(2)–C(10)–C(9)	114.0 (7)
Cu(1)–O(2)–Cu(2)	98.2 (2)	O(3)–C(12)–O(4)	129.2 (7)
Cu(1)–O(2)–C(14)	131.8 (5)	O(3)–C(12)–C(13)	113.5 (7)
Cu(2)–O(2)–C(14)	125.2 (5)	O(4)–C(12)–C(13)	117.3 (7)
Cu(2)–O(3)–C(12)	127.5 (5)	O(2)–C(14)–O(5)	122.0 (7)
Cu(1)–O(4)–C(12)	130.3 (5)	O(2)–C(14)–C(15)	119.6 (7)
C(3)–O(6)–C(16)	118.5 (6)	O(5)–C(14)–C(15)	118.4 (7)

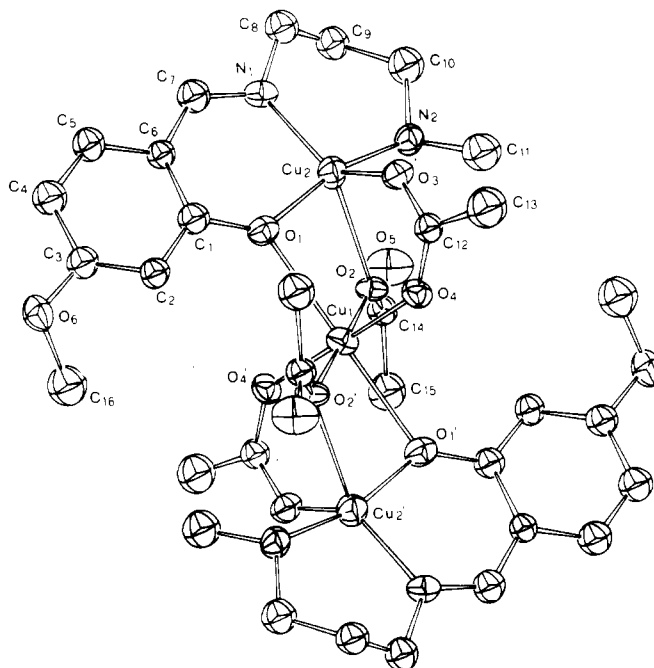


**Figure 1.** View of the trinuclear  $\text{Cu}_3\text{L}_2(\text{CH}_3\text{COO})_4$  molecule. Hydrogen atoms have been omitted for clarity. Unlabeled atoms are related to labeled atoms by the inversion center.

15 for Cu; the correction for anomalous dispersion of Cu was included.

## Results

**Description of the Structure.** The crystal structure consists of trinuclear units of formula  $\text{Cu}_3\text{L}_2(\text{CH}_3\text{COO})_4$ . Final positional

(13) Walker, N.; Stuart, D. *Acta Crystallogr., Sect. A: Found. Crystallogr.* **1983**, *A39*, 158.

(14) Sheldrick, G. M. "SHELX-76, Program for Crystal Structure Determination"; University of Cambridge: Cambridge, England, 1976.

(15) "International Tables for X-ray Crystallography"; Kynoch Press: Birmingham, England, 1974; Vol. IV, p 99.

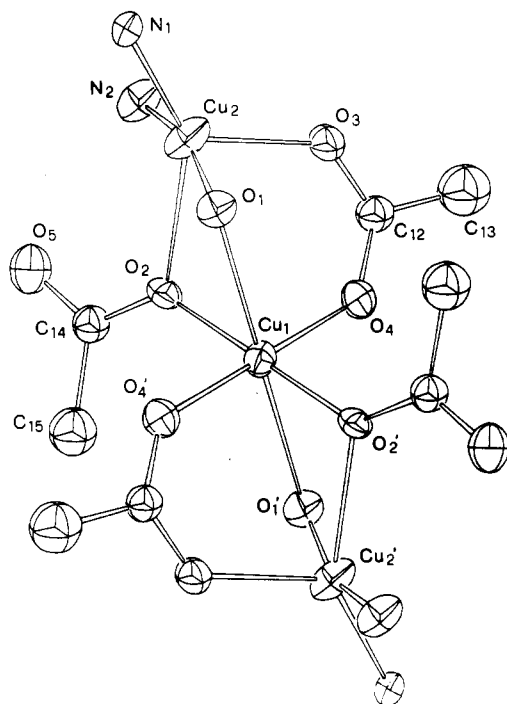


Figure 2. Schematic view of the bridging framework in  $\text{Cu}_3\text{L}_2(\text{CH}_3\text{COO})_4$ .

parameters are listed in Table I, the more important interatomic distances and bond angles are compiled in Table II, and least-squares planes are collected in Table III (supplementary material). The structure of the compound is presented in Figures 1 and 2.

Intermolecular contacts between non-hydrogen atoms of the trinuclear units are always longer than the sums of van der Waals radii, suggesting that the individual trimers in the structure are effectively isolated.

The compound has  $\bar{1}$  crystallographic symmetry, with Cu(1) located on a center of symmetry.

The sites of the central and terminal copper ions are non-equivalent. The coordination sphere of the central copper atom,  $\text{CuO}_6$ , has a symmetry close to  $D_{4h}$ , with four strong bonds (1.943 (6) and 2.000 (5) Å) forming an exact plane and two weak axial bonds (2.533 (7) Å), to O(1) and O(1)', that form an angle of  $73.5^\circ$  with that plane. The two outer copper atoms are five-coordinate and have an identical ligand environment,  $\text{CuN}_2\text{O}_3$ , owing to crystallographic inversion symmetry. The Cu(2)–O(2) bond (2.377 (7) Å) is considerably longer than any of the other Cu(2)–N (2.091 (9) and 2.007 (7) Å) or Cu(2)–O (1.923 (5) and 2.076 (6) Å) bonds. Atoms Cu(2), N(1), O(2), and O(3) lie only between 0.01 and 0.06 Å from a plane calculated for these four atoms. The Cu(2)–O(1) and Cu(2)–N(2) bonds form angles of 82 and  $81^\circ$ , respectively, with that plane.

The gross structure about the outer copper atoms can be visualized as being derived from a trigonal-bipyramidal arrangement by having one equatorial donor atom O(2), moved away from the copper ion and the two axial donor atoms, O(1) and N(2), bent toward O(2) (the O(1)–Cu(2)–O(2) and N(2)–Cu(2)–O(2) angles are  $79.3$  (2) and  $84.0$  (2)°, respectively). The principal departure from trigonal-bipyramidal coordination arises from the deviations from the regular value of  $120^\circ$  of the angles generated in the equatorial plane by O(2), O(3), and N(1) with Cu(2):  $124.3$  (2),  $144.4$  (2), and  $90.9$  (2)°. The coordination geometry of Cu(2), which is similar to that observed in the structure of e.g.  $[(\text{C}_2\text{H}_5)_2\text{CHNH}_2]_2\text{CuCl}_4$ ,<sup>16</sup> can be described<sup>2b</sup> as lying on a geometric reaction path that relates a trigonal bipyramid to a distorted tetrahedron and a separate donor atom.

An alternative description of the geometry around Cu(2) based on a square pyramid with O(2) occupying the axial position and

ENERGY	$S$	$S^*$	$g$
$-\frac{1}{2}J'$	3/2	1	$(1/3)(g_1+g_2+g_2') = g_a$
$(2/3)J'$	1/2	0	$g_1 = g_b$
$2J - (1/2)J'$	1/2	1	$(2/3)g_2 - (1/3)g_1 + (2/3)g_2' = g_c$

Figure 3. Energies and  $g$  tensors (expressed as linear combinations of the  $g$  tensors of the individual ions) of the spin states for a linear trinuclear copper(II) compound with two equivalent copper ions.

O(1), O(3), N(1), and N(2) defining the basal plane is not considered to be significant since the latter atoms deviate from planarity by no less than 0.6 Å.

There are two types of bridges between each pair of adjacent copper ions in the trimer: a Cu–O–C–O–Cu acetate bridge and a four-membered  $\text{Cu}_2\text{O}_2$  ring involving a one-atom bridging acetate group and the phenolic oxygen of tridentate  $\text{L}^-$ .

Atoms Cu(1), O(4), C(12), O(3) and Cu(2) lie approximately on a plane, the maximum deviation from planarity being 0.16 Å. This plane forms dihedral angles of  $147^\circ$  with the equatorial plane of the distorted trigonal bipyramid around Cu(2) and of  $134^\circ$  with the plane of the square around Cu(1).

The four-membered  $\text{Cu}_2\text{O}_2$  ring is highly asymmetric and involves four different bond lengths and four different bond angles. Angles at O(1) and O(2) are  $95.3$  (2) and  $98.2$  (2)°, respectively. The larger angle corresponds to the more strongly linked superexchange pathway. The dihedral angle between the Cu(1)–O(1)–O(2) and Cu(2)–O(1)–O(2) planes is  $7.6^\circ$ . The equatorial plane of the distorted trigonal bipyramid around Cu(2) forms a dihedral angle of  $104^\circ$  with the plane of the square around Cu(1).

Bond distances and angles of the  $\text{L}^-$  ligand are normal. A rather loose contact of 2.855 (9) Å between the noncoordinated oxygen of the monodentate acetate group, O(5), and N(2) may be indicative of some hydrogen-bonding interaction. The Cu...Cu separation between nearest neighbors is 3.319 (1) Å.

**Magnetic Properties.** Before presenting the magnetic results, we will briefly sketch the theoretical background requisite to make the following discussion clearer.

A spin Hamiltonian appropriate to describe the exchange interaction in a linear symmetric copper(II) trimer like  $\text{Cu}_3\text{L}_2(\text{C}_2\text{H}_3\text{COO})_4$  has the form<sup>17</sup> shown in eq 1, where  $J$  describes the

$$\hat{H}_{ex} = -2J(\hat{S}_1 \cdot \hat{S}_2 + \hat{S}_1 \cdot \hat{S}_2') - 2J'(\hat{S}_2 \cdot \hat{S}_2') \quad (1)$$

interaction between adjacent copper ions and  $J'$  describes the interaction between the outer copper ions. The subscripts refer to the metal ions as indicated in Figure 2. Defining the spin operators  $\hat{S} = \hat{S}_1 + \hat{S}_2 + \hat{S}_2'$  and  $\hat{S}^* = \hat{S}_2 + \hat{S}_2'$ , Figure 3 portrays schematically the resulting spin states (labeled according to the  $S$  and  $S^*$  quantum numbers), their energies, and the  $g$  tensors of the various multiplets expressed as linear combinations<sup>2f,8,18,19</sup> of the  $g$  tensors of the individual ions. In an external magnetic field each multiplet is split into  $2S + 1$  components that are separated by  $g_i\beta H$ , where  $g_i$  is the Landé splitting factor for that multiplet. Assuming a Boltzmann distribution for the population of the quartet and doublet states, the molar susceptibility is given by eq 2, where  $X = \exp(J/kT)$ ,  $Y = \exp(J'/2kT)$ ,  $Z_i = \exp$

$$\chi_M = (N\beta/2H)\{g_c X^{-2}(Z_c - Z_c^{-1}) + g_b Y^{-4}(Z_b - Z_b^{-1}) + g_a X[3(Z_a^3 - Z_a^{-3}) + (Z_a - Z_a^{-1})]\}/\{X^{-2}(Z_c + Z_c^{-1}) + Y^{-4}(Z_b + Z_b^{-1}) + X[(Z_a^3 + Z_a^{-3}) + (Z_a + Z_a^{-1})]\} \quad (2)$$

$(g_i\beta H/2kT)$ , and the other symbols have their usual meaning. With the assumption that the  $g$  values for all three copper atoms are equal, eq 2 reduces to eq 3. If it is further assumed that  $g\beta H$

$$\chi_M = (Ng\beta/2H)\{(X^{-2} + Y^{-4})(Z - Z^{-1}) + X[3(Z^3 - Z^{-3}) + (Z - Z^{-1})]\}/\{(X^{-2} + Y^{-4})(Z + Z^{-1}) + X[(Z^3 + Z^{-3}) + (Z + Z^{-1})]\} \quad (3)$$

(17) Griffith, J. S. *Struct. Bonding (Berlin)* 1972, 10, 87.

(18) Scaringe, J.; Hodgson, D. J.; Hatfield, W. E. *Mol. Phys.* 1978, 35, 701.

(19) Kokoszka, G. F.; Duerst, R. W. *Coord. Chem. Rev.* 1970, 5, 209.

(16) Anderson, D. N.; Willett, R. D. *Inorg. Chim. Acta* 1974, 8, 167.

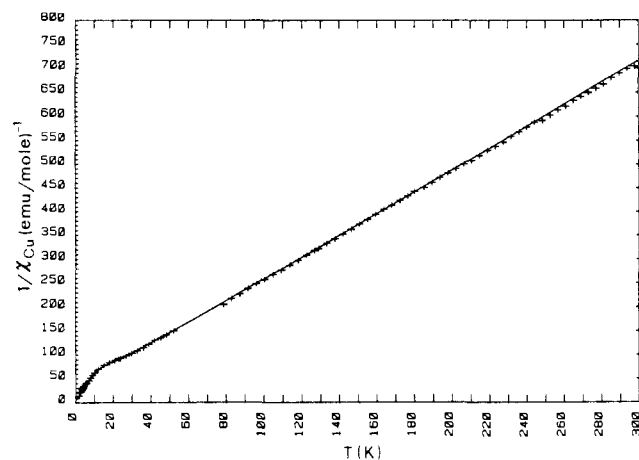


**Figure 4.** Reciprocal magnetic susceptibility (per copper ion) vs. temperature for  $\text{Cu}_3\text{L}_2(\text{CH}_3\text{COO})_4$ . Experimental points are shown as crosses. The full line through the data represents the best fit with  $J = -9.7 \text{ cm}^{-1}$ ,  $J' = -2.7 \text{ cm}^{-1}$ , and  $g = 2.15$ .

$\ll kT$ , eq 4, which is the most commonly used in the literature, is obtained.

$$\chi_M = (N\beta^2 g^2 / 4kT)(X^{-2} + Y^{-4} + 10X) / (X^{-2} + Y^{-4} + 2X) \quad (4)$$

The temperature variation of the inverse susceptibility (per copper ion) of  $\text{Cu}_3\text{L}_2(\text{CH}_3\text{COO})_4$  in the temperature range ca. 2–300 K is shown in Figure 4. The plot is linear above ca. 30 K, exhibits a shoulder between 10 and 30 K, and is again approximately linear below ca. 10 K. The high-temperature data extrapolate to a Curie-Weiss  $\Theta$  value of  $-14.1 \text{ K}$ , with a Curie constant of  $0.43 \text{ cgsu K}$ , and hence a  $g$  value of 2.15. The low-temperature data extrapolate to a Curie-Weiss  $\Theta$  value not significantly different from zero.

The effective magnetic moment per trimer is  $3.19 \mu_B$  at 298 K, a value appropriate for three virtually independent copper ions (when  $kT$  is much larger than  $J$ ,  $J'$ , and  $g\beta H$ ,  $\chi_M$  reduces to the sum of the susceptibilities of three independent copper(II) ions), decreases between ca. 300 and 10 K, and becomes almost constant below ca. 10 K with a value of  $1.73 \pm 0.04 \mu_B$ , appropriate for a system with a spin  $1/2$  ground state.

The room-temperature X-band ESR spectra of polycrystalline samples of the compound show only one broad (peak-to-peak separation ca. 400 G) uninterpretable signal centered at  $g = 2.14$ . Decreasing the temperature of the sample to 77 K leads to a slightly narrower signal (peak-to-peak separation ca. 300 G) centered at  $g = 2.11$ . There were no additional features (Cu hyperfine, zero-field splitting, or half-field  $\Delta M_s = 2$  transition) from one temperature to the other.

Eq 3 was used to fit the experimental susceptibility data. The  $g$  value of 2.15, deduced from the higher temperature "paramagnetic" region susceptibility data, was held constant during all fitting calculations. In the absence of adequate information about the "molecular"  $g$  values, eq 2 provides too many parameters for reasonable evaluation. On the other hand, eq 3 is more correct than eq 4 in the low-temperature region, where the  $g\beta H$  (ca.  $1 \text{ cm}^{-1}$  for  $H = 10000 \text{ G}$ ) and  $kT$  terms are of comparable magnitude. The function that was minimized in curve fitting was  $F = (\chi_i^{\text{obsd}} - \chi_i^{\text{calcd}})^2 (\chi_i^{\text{obsd}})^{-1}$ .

The  $J$  and  $J'$  parameters show a strong correlation with each other. Curve A in Figure 5 shows how the best  $J$  and  $J'$  values, at the  $g$  value of 2.15, are correlated. The intersections of a vertical line with curves A and B give the value of the agreement factor  $F$  (curve B) for a given set of  $J$  and  $J'$  values (curve A). The two minima in curve A correspond to  $J = -9.7$ ,  $J' = -2.7 \text{ cm}^{-1}$  and  $J = -5.1$ ,  $J' = -12.0 \text{ cm}^{-1}$ , respectively ( $F = 1.476 \times 10^{-2}$  for 93 observations). However, even for  $J = -10.2$ ,  $J' = 0.0 \text{ cm}^{-1}$  the resulting best fit differs little from that obtained with the former sets of parameters. The full line through the data in Figure 4 represents the best fit with  $J = -9.7$ ,  $J' = -2.7 \text{ cm}^{-1}$ .

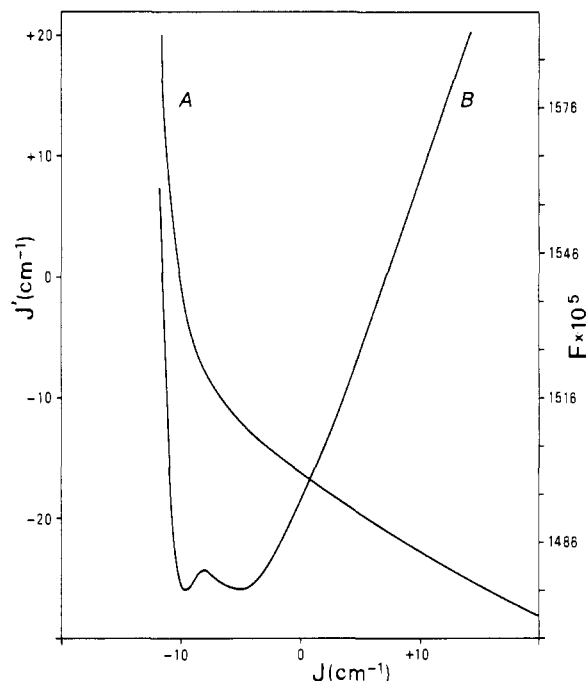


**Figure 5.** Correlation plot between the  $J$  and  $J'$  parameters at a  $g$  value of 2.15. The intersections of a vertical line with curves A and B give the value of the agreement factor  $F$  (curve B) for a given set of  $J$  and  $J'$  values (curve A).

There is no set of coupling constants that would be consistent with antiferromagnetic coupling between adjacent copper ions and ferromagnetic coupling between terminal copper ions.

To conclude, the present results only allow us to say that there is a rather weak antiferromagnetic interaction ( $-J = \text{ca. } 5\text{--}10 \text{ cm}^{-1}$ ) between nearest neighbors and that if end-to-end coupling is present, it is antiferromagnetic.

## Discussion

The temperature dependence of the magnetic susceptibility data for  $\text{Cu}_3\text{L}_2(\text{CH}_3\text{COO})_4$  has a form appropriate for an antiferromagnetically coupled copper(II) linear trimer; when the temperature is lowered, the effects of the depopulation of the quartet state and the consequent population of the lower doublet states (or state) are clearly discernible. However, the analysis of the magnetic data with eq 3 fails to provide accurate values of the exchange parameters, due to the equal or comparable "best fits" that are obtained with different sets of  $J$  and  $J'$  values, in particular with both  $J' = 0$  and  $J' \neq 0$ .

The correlation between the  $J$  and  $J'$  parameters in determining the temperature dependence of the theoretical magnetic susceptibility for linear copper(II) trimers has been noted previously by other authors<sup>8,10</sup> and is an inherent feature of the theoretical model represented by eq 3 and 4. This unsatisfactory feature is commonly circumvented by assuming only nearest-neighbor interactions, on the basis of the necessarily long orbital pathway that links the terminal ions in a linear trimer. However, this practice is difficult to justify in light of the rapidly increasing number of reported compounds<sup>24,20,21</sup> in which significant magnetic exchange coupling is propagated up to distances in excess of 6–10 Å.

In the present case, the main weakness in the analysis of the magnetic data seems to be the assumption of equal  $g$  values for all three copper ions, in other words the use of eq 3 instead of eq 2, which allows different  $g$  values for the various multiplets and hence different weights of the populations of the quartet and doublet states. The expressions in Figure 3 show that the  $g$  values

(20) Chiari, B.; Piovesana, O.; Tarantelli, T.; Zanazzi, P. F. *Inorg. Chem.* **1984**, *23*, 2542.

(21) Chiari, B.; Hatfield, W. E.; Piovesana, O.; Tarantelli, T.; ter Haar, L. W.; Zanazzi, P. F. *Inorg. Chem.* **1983**, *22*, 1468.

of the spin doublets and of the spin quartet are different provided that the  $g$  values of the individual ions are different. This is likely to be the case here in light of the markedly different geometries (ground states) that are observed for the central and outer copper ions. An independent, low-temperature single-crystal ESR investigation of the molecular  $g$  values appears to be needed in order to improve the interpretation of the exchange interaction in the present compound. Work in this direction is being attempted.

Meanwhile, it is of some interest to scrutinize whether the rather small magnitude of the magnetic coupling ( $-J = \text{ca. } 5\text{--}10 \text{ cm}^{-1}$ ) that is observed between adjacent copper ions may be related to the nature of the magnetic orbitals on Cu(1) and Cu(2) and the geometrical features of the  $\text{Cu}_2\text{O}_2$  and  $\text{Cu-O-C-O-Cu}$  bridges.

Cu(1) has an elongated tetragonal geometry close to  $D_{4h}$ . In this symmetry the unpaired electron of the copper ion lies in the  $b_{1g}$  ( $d_{x^2-y^2}$ ) orbital, and there is practically no unpaired electron density on the axial ligands O(1) and O(1)'. On the other hand, Cu(2) has a distorted geometry falling between trigonal bipyramidal and tetrahedral, which complicates knowing which orbital has the unpaired electron. For reasons discussed in detail above we believe that the trigonal-bipyramidal assignment is a more accurate one for Cu(2). If this is the case, the unpaired electron resides primarily in a  $d_{z^2}$  type orbital and will be delocalized out both on the axial (O(1), N(2)) and on the equatorial ligands (O(2), O(3), N(1)), but certainly less on the latter.

There are very few structurally characterized complexes that contain four-membered  $\text{Cu}_2\text{O}_2$  rings with nonequivalent copper sites.<sup>22</sup> In the recently reported<sup>22</sup>  $[\text{Cu}_2(\text{N}_3\text{O})\text{OH}][\text{BF}_4]$  complex (whose copper ions are bridged by phenolate and hydroxo groups), one copper resides in a square-pyramidal geometry while the other is closer to a trigonal-bipyramidal arrangement. The magnitude of the magnetic coupling in this compound is quite large,  $J = -210 \text{ cm}^{-1}$ , and the orientation of the copper ions is such that the orbitals containing the unpaired electrons have high electron density along the bridging bonds. In the  $\text{Cu}_2\text{O}_2$  ring of the present complex there is practically no unpaired electron density along the Cu(1)-O(1) bond. Exchange coupling of the copper ions must result essentially from overlap through the one-atom acetate bridge, O(2), and this overlap is most likely to be small because of both the small unpaired electron density in the equatorial plane around Cu(2) and the long Cu(2)-O(2) distance, 2.377 (7) Å. The effect of the bridging angle at O(2), 98.2 (2)°, may be predicted to play a minor role in light of the nondirectional character of the unpaired electron density in the equatorial plane of Cu(2).

Structural and magnetic data are available for more than 40 copper(II) carboxylates with a bridged dinuclear structure. The  $J$  values for these compounds, which contain four bridging ligands, vary from  $-108 \text{ cm}^{-1}$  to approximately  $-250 \text{ cm}^{-1}$ .<sup>23</sup> Many attempts have been made to correlate the magnetic behavior ( $J$  values) with structural and physical properties; however, success has only been limited.<sup>24,23</sup> The much smaller interaction supported by the  $\text{Cu-O-C-O-Cu}$  acetate bridge ( $<|5\text{--}10| \text{ cm}^{-1}$ ) in  $\text{Cu}_3\text{L}_2(\text{CH}_3\text{COO})_4$  can be justified on several grounds. E.g., in the trimer there is only one three-atom bridge between nearest neighbors, and in addition, the  $\text{Cu-O-C-O-Cu}$  superexchange path distance, 6.551 Å, is significantly longer than the corresponding distances observed for the cupric carboxylates, 6.42–6.44 Å.<sup>23</sup> Further, in the cupric carboxylates the unpaired electron density of both the copper ions is in  $d_{x^2-y^2}$  orbitals pointing toward the oxygen atoms, a feature that in the present case applies to Cu(1) but not to Cu(2). If Cu(2) is close to a trigonal-bipyramidal geometry, the unpaired electron density along the Cu(2)-O(3) bond, which lies in the equatorial plane, should be considerably reduced with respect to the case of the cupric carboxylates or the Cu(1)-O(4) bond. The fact that the Cu(2)-O(3) bond distance, 2.076 (6) Å, is significantly longer than the Cu(1)-O(4) distance, 1.943 (6) Å, and any of the Cu-O(basal) distances observed for the cupric carboxylates (in the range 1.96–1.97 Å)<sup>23</sup> is in agreement with this view.

In conclusion, the molecular structure of  $\text{Cu}_3\text{L}_2(\text{CH}_3\text{COO})_4$  indicates that both the orbital pathways that are available for magnetic exchange between adjacent copper ions are rather ineffective in yielding a sizable coupling. This concept is in agreement with the small magnitude of the antiferromagnetic interaction that is observed.

**Acknowledgment.** Magnetic measurements were made in the laboratory of Professor William E. Hatfield, The University of North Carolina at Chapel Hill. O.P. thanks Professor Hatfield for his hospitality and expresses his appreciation to Mr. Jeffrey H. Helms for his valuable assistance in securing the magnetic measurements.

**Registry No.**  $\text{Cu}_3\text{L}_2(\text{CH}_3\text{COO})_4$  (L = *N*-methyl-*N'*-(4-methoxysalicylidene)-1,3-propanediamine), 99248-57-4; *N*-methyl-1,3-propanediamine, 6291-84-5; 2-hydroxy-4-methoxybenzaldehyde, 673-22-3.

**Supplementary Material Available:** Listings of mean planes and atomic displacements (Table III), thermal parameters (Table IV), hydrogen atom coordinates (Table V), and observed and calculated structure factor amplitudes (9 pages). Ordering information is given on any current masthead page.

(22) Sorrell, N. T.; Jameson, D. L.; O'Connor, C. J. *Inorg. Chem.* **1984**, *23*, 190 and references therein.

(23) Melnik, M. *Coord. Chem. Rev.* **1982**, *42*, 259 and references therein.